A Novel Mathematical Model Identifies Potential Factors Regulating Bone Apposition

M. J. Martin, J. C. Buckland-Wright

Applied Clinical Anatomy Research, School of Biomedical Sciences, King's College, London, United Kingdom

Abstract. The development of pharmaceutical treatments for bone disease can be enhanced by mathematical models that predict their effects on matrix apposition during cancellous bone remodelling. Therefore, a mathematical model was constructed to simulate the rate of focal bone formation from the number of osteoid-forming osteoblasts at one microsite and their rate of activity. The number of mature osteoid-forming cells was simulated from a relationship describing the proliferation of preosteoblasts. Osteoblast activity was described by Michaelis-Menten enzyme kinetic equations adapted to describe cellular activity. The model incorporates the negative feedback effects on the rates of bone apposition due to the reduction in size of mature osteoblasts with continuing differentiation and the reduction in number of osteoid-forming cells with apoptosis and osteocyte formation. In addition, the rate of mineralisation is limited according to osteoid substrate availability. Results of sensitivity analysis revealed the amount of bone formed at one microsite to be more sensitive to changes in factors that controlled cell growth during proliferation and the number of mature osteoid-forming osteoblasts than to those that determined cellular activity. Matrix and osteocyte signalling were shown to have potentially important roles in controlling rates of osteoid apposition in normal, healthy bone. This simple model supports the critical role of controlled mitotic growth in normal bone apposition. It can also help to explain how the homeostatic processes of bone resorption and apposition during remodelling can be disrupted by growth factors that affect the mitotic fraction and division time of proliferative preosteoblast cells.

Key words: Osteoblast — Proliferation — Apposition — Michaelis-Menten equation — Control mechanism

The development of pharmaceutical treatments for bone disease can be enhanced by mathematical models that predict their effects on bone apposition. However, the rate of bone apposition depends on the number and the activity of osteoblasts, both of which change as apposition progresses [1, 2]. During the reversal phase in the remodelling of healthy cancellous bone, committed osteoprogenitor stem cells migrate from the bone marrow to the surface of newly excavated matrix, where they undergo proliferation and differentiation. By the end of the proliferative phase, the preosteoblasts have differentiated into tall columnar, mature collagen-producing osteoblasts [1, 2]. The densely packed osteoblasts change shape and continue to differentiate as they deposit new osteoid. After a lag time of approximately 15 days, the osteoid is mature enough for mineralisation to begin [2, 3]. Some osteoblasts become embedded within the mineralised matrix to form new osteocytes, thereby adding to the interconnecting network of osteocytes within the matrix. Meanwhile, those osteoblasts that remain on the bone surface become progressively flatter, longer, and less columnar, finally forming a layer of lining cells covering the surface of the new matrix at the end of the formation phase of remodelling [1, 3]. During bone apposition, the number of osteoid-forming cells is reduced by both osteocyte formation and apoptosis. Cell size decreases, which reduces cell volume and the amount of endoplasmic reticulum and Golgi apparatus available for collagen protein synthesis. Decreases in both cell number and size contribute to a progressive reduction in osteoid formation and mineralisation [2, 4]. Predicting the effects of pharmaceutical treatments on bone formation will therefore require robust mathematical models, based on underlying biological processes, that are able to account for the cell growth during proliferation and the negative feedback effects caused by gradual reduction in the number of cells and their size.

In other fields of endocrinology, the Michaelis-Menten (M-M) kinetic equations of enzyme activity have been adapted to describe rates of cellular activity [5, 6]. M-M equations also underlie process-based models in fields of biology that predict outcomes from complex interactive factors, such as the well-validated mechanistic models of photosynthesis [7, 8], which have

---

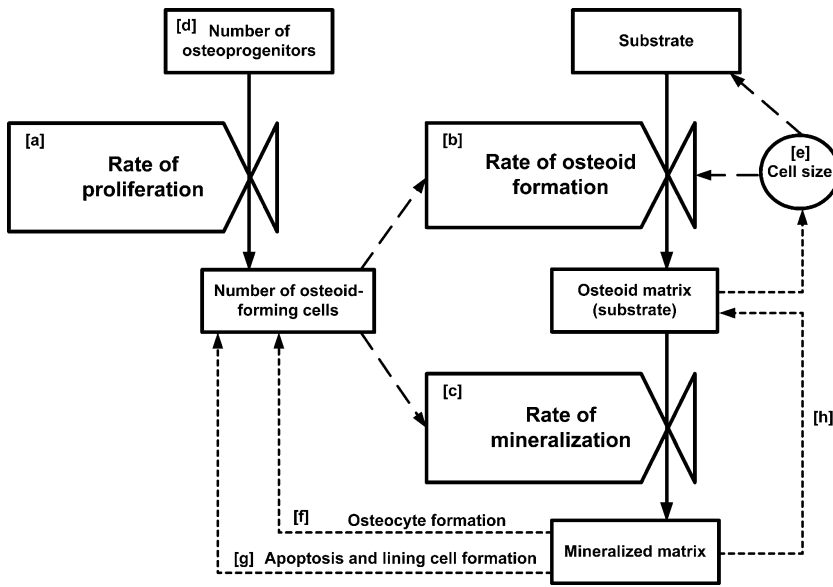*Correspondence to:* M. J. Martin; E-mail: marion.martin@kcl.ac.uk

Fig. 1. Model relational diagram, where **a-c** are the three rate variables, **d** and **e** are the state and auxiliary variables (number of osteoprogenitor cells and cell size, respectively), and **f-h** are the three feedback effects. The fourth feedback effect (not shown) is the autoregulated reduction in cell size that accompanies differentiation. *Solid lines* represent flow of matter and *dashed lines* represent flow of information; *small dashed lines* represent feedback effects.

been adapted and scaled up to predict effects of environmental factors on plant physiology and productivity [9–12]. In bone, other mathematical models have been formulated to simulate processes at the trabecular or basic multicellular unit (BMU) level [13–16]. We have previously used M-M equations to simulate changes in cellular activity to describe bone resorption during remodelling [17]. As far as we can ascertain, no attempt has been made to predict the depth and duration of bone apposition using such equations.

The objectives of this work were twofold. The first was to construct a mathematical model that predicted the amount of bone formed during remodelling in healthy adult cancellous bone, based on changes in cell number and cellular activity. This model used a relationship that describes the proliferation of muscle stem cells [18] to calculate the initial number of osteoid-forming cells and M-M equations to describe changes in the rates of cellular activity, based on matrix and mineral apposition rates of normal healthy cancellous bone determined by histomorphometric techniques [3]. Second, sensitivity analysis was used to identify factors that potentially regulate bone apposition and so assist the development of therapeutic treatment of bone-related disease and cancer-induced metastasis to bone.

Methods

Model Overview

Attempts at *in vivo* investigation of bone biology necessarily disrupt the very processes that are being measured. In lieu of *in vivo* data, a model was constructed using information on cellular activity during bone apposition gained from published histomorphometric studies. The principles of the bone apposition model are outlined in Figure 1, with equations derived from the literature as described below. The model was based on three cellular process rates: the rate of proliferation of preosteoblasts (Fig. 1a), the rate of osteoid-forming cellular activity (Fig. 1b), and the rate of mineralising cellular activity (Fig. 1c).

As the number of osteoblast lineage cells is crucial in determining the rate of bone formation at one microsite and the aim of this work was to base this model on as much biological information as possible, the proliferation of preosteoblasts during phase III was based on a relationship that describes the proliferation of muscle stem cells in the presence of different growth factors [18]. The rates of osteoid apposition (Fig. 1b) and mineralisation (Fig. 1c) were described by M-M equations, which simulate the rate of an enzyme catalysed reaction in a homogeneous medium, adapted to describe rates of cellular activity (*A*) as follows:

$$A = (V_{max} \cdot s)/(s + K_m) \qquad (1)$$

where V_{max} is the maximum velocity of cellular activity, s is the amount of substrate available, and K_m is the M-M constant. The M-M constant is equal to the amount of substrate when activity equals half the maximum rate. The rate of cellular activity refers to the function that is being simulated. Thus, for the purpose of this model, A_{Ost} represented the rate of osteoid-forming activity and A_{Mz} represented the rate of mineralisation. Mature osteoblasts produce collagen to form the osteoid matrix, which takes approximately 15 days to mature [3]. This matrix maturation phase (phase IV, for explanation of the separate phases of remodelling refer to Fig. 2) is followed by phase V. During phase V, osteoblasts control the mineralisation of the older, mature osteoid at the same time as continuing to form new osteoid, although at a much reduced rate [3]. Indeed, at the start of phase V, when osteoblasts are involved in both mineralisation and osteoid formation, the rate of osteoid formation is reduced by approximately 50% of the rate at the start of phase IV (see Fig. 8h of Eriksen et al. [3]). Phase V is followed by a return to quiescence (phase 0), until remodelling is activated once again [1, 2].

Concurrent with the process described above, negative feedback effects reduce both cell number and activity during bone apposition. The following feedback effects are incorporated within the model.

1. During phases IV and V, osteoblasts continue to differentiate, becoming flatter, longer cells. This autoregulated
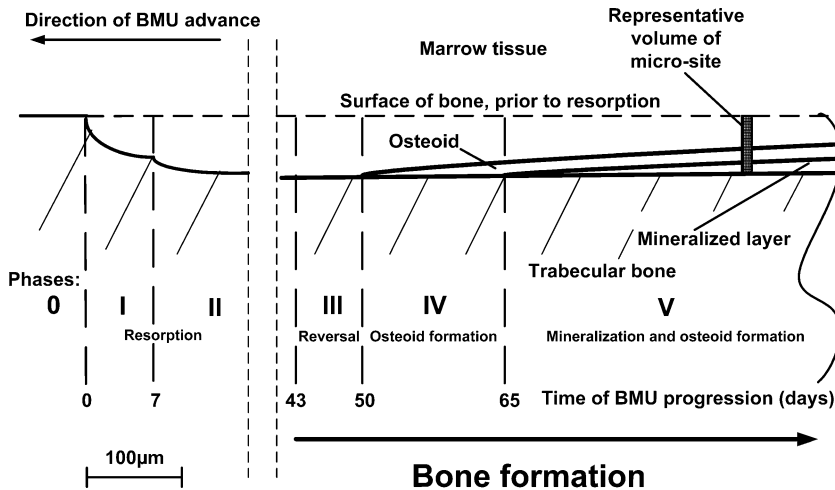
Fig. 2. Schematic of progression of a BMU across the surface of trabecular bone to illustrate the relationship between the phases of formation during remodelling and the representative microsite unit (*shaded area*).

reduction in cell size is accompanied by a reduction in endoplasmic reticulum and Golgi apparatus, which was assumed, for model purposes, to limit the maximum capacity of cellular osteoid-forming activity ($V_{\mathrm{max,Ost,0}}$) (Fig. 1e).

2. During phase V, the number of active osteoblasts is reduced by osteocyte formation (Fig. 1f). The number of active cells is further reduced by enhanced apoptosis. Although apoptosis of osteoblasts may occur at any stage of matrix apposition, during phase V apoptosis rates are enhanced to remove excess cells that are not required for either lining cell or osteocyte formation (Fig. 1g).

3. Finally, during the late stages of phase V, the availability of osteoid substrate has a feedback effect upon the rate of mineralisation (Fig. 1h).

Although the three-dimensional remodelling of a complete BMU involves horizontal progression of an osteoblast front across the surface of trabeculae [19], remodelling at each microsite within a BMU can be considered to be a down-up process, where different types of bone cell actively remove and then replace bone. Therefore, in order to simulate cellular activity during formation, the area covered during 1 day's horizontal progression of a BMU was chosen to denote the representative area of a "microsite" (Fig. 2), thus allowing the results of cellular activity during focal bone formation to be simulated as a seam depth, or seam apposition, phenomenon. The daily time step was considered appropriate in view of both the time taken to completely remodel one microsite (estimated as 195–200 days [20, 21]) and the need to be able to disregard the shorter-term fluctuations. The area of the microsite was estimated to be 6,500 μm², based on the mean width of a BMU (650 μm) [22] and the horizontal progression of a BMU (10 μm/day) [2, 21]. For full details of the derivation of dimensions for the microsite, please refer to Martin and Buckland-Wright [17].

The model was programmed in Microsoft (Redmond, WA) Visual Basic™ to simulate the changes in seam depth during formation at one microsite on a daily time step, using cell proliferation rates described by Deasy et al. [18] to determine cell number and M-M equations to simulate changing rates of osteoid apposition and mineralisation. Numerical values of the model variables were estimated by comparing model simulations against changes in matrix and mineral apposition and relative changes in osteoid thickness, calcification rate, and matrix apposition rate (as illustrated in Figs. 7 and 8B,D,H of Eriksen et al., respectively [3]). Model simulations of the change in depth of apposition and mineralisation are shown by the dashed and solid lines of Figure 3, respectively. The model outputs were the number of mature osteoblasts formed by the end of phase III, the depth of osteoid formation, the depth of mineralisation, and the duration of the formation phases (IV
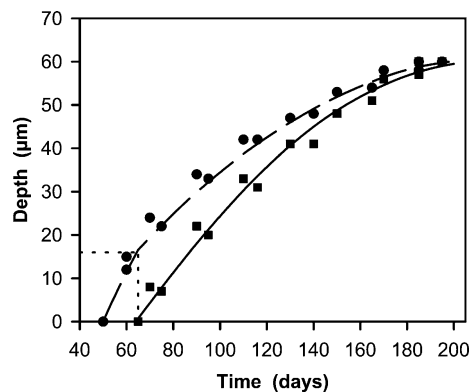

Fig. 3. Simulated change in depth of osteoid apposition (*dashed line*) and mineralisation (*solid line*) during phases IV and V, using input values listed in Table 2, compared with the data of osteoid apposition (*circles*) and mineralisation (*squares*) from Figure 7 in Eriksen et al. [3], used for model construction. *Time in days* refers to time from origination of remodelling.

and V in Fig. 2). Model construction is described in greater detail below.

Model Construction

Phase III: Preosteoblastic proliferation. The growth in the number of osteoblast lineage cells was simulated by the relationship that describes the growth in the number of muscle stem cells under the influence of different growth factors [18] [equation 2 in Table 1, where N_0 is the number of committed osteoprogenitor cells at the start of proliferation, α is the mitotic fraction (which is the proportion of cells that are capable of undergoing cell division), and T is the division time (i.e., the total duration between the onset of successive divisions)]. All model symbols are defined in Table 2. Values for mitotic fraction and division time were the same as those used by Deasy et al. [18]. Also, the number of osteoblast lineage cells present on day 1 of phase III was assumed to be five, which is consistent with the data from Deasy et al. [18], who started with four to six cells in their experiments. Thus, 6 days later, after nine divisions, the total number of mature osteoblasts formed by the end of phase III was 286. Although in reality cell size and cell density might be expected to vary from site to site, the 286 cells simulated by the model was consistent with a guide number of between 100 and 400 osteoblasts per bone-forming site [23] and gave a cell density within the order of

Table 1. Model equations

$$N = N_0\{0.5 + [1 - 2\alpha^{(t \times 24/T + 1)}]/(2 - 4\alpha)\} \tag{2}$$

$$t = P_{Ost}$$

$$G_{Ost} = \Sigma A_{Ost} \tag{3}$$

$$t = 0$$

$$A_{Ost} = [V_{max,Ost} \cdot s_{Ost}/(s_{Ost} + K_{m,Ost})] \cdot N \tag{4}$$

$$V_{max,Ost,t+1} = V_{max,Ost,t-z} \tag{5}$$

$$t = P_{Mz}$$

$$G_{Mz} = \Sigma A_{Mz} \tag{6}$$

$$t = 0$$

$$A_{Mz} = [V_{max,Mz} \cdot s_{Mz}/(s_{Mz} + K_{m,Mz})] \cdot N \tag{7}$$

Symbols are described in Table 2.

magnitude expected for tall columnar osteoblasts. By the end of phase III, all preosteoblasts have become mature, column-shaped osteoblasts [3].

Phase IV: Osteoid formation and maturation. The fully mature osteoblasts secrete the collagen that forms the new osteoid matrix together with growth factors, such as transforming growth factor-ß (TGF-ß), platelet-derived growth factor (PDGF), and fibroblast growth factor (FGF), which are incorporated within the matrix [24]. The mature osteoblasts contain well-developed rough endoplasmic reticulum and extensive Golgi apparatus [23], which are necessary for protein synthesis. The accumulated growth of osteoid (G_{Ost}) was calculated on a daily time step (equation 3 in Table 1, where A_{Ost} is the osteoid-forming osteoblast activity per day and P_{Ost} is the period of osteoid apposition). The daily activity of osteoblasts was described in the model by M-M kinetics (equation 4 in Table 1, where $V_{max,Ost}$, s_{Ost}, and $K_{m,Ost}$ are the maximum rate of osteoid-forming activity, the substrate, and the M-M constant of osteoid formation, respectively). The substrate s_{Ost} represents the blood's supply of amino acids for protein synthesis. The M-M equation therefore represented the activity per cell, and this was multiplied by the number of mature osteoblasts (N) to determine the osteoid formation activity at the microsite level.

The values of the M-M input parameters $V_{max,Ost}$ and $K_{m,Ost}$ were estimated from the maximum rate of osteoid formation [2, 3], which was assumed to be equal to the initial rate of matrix apposition of 1.2 µm/day [2] (as illustrated in Fig. 7 of Eriksen et al. [3]). In lieu of data on substrate uptake, the input value of s_{Ost} was estimated as 200 from the dose-response curve of relative alkaline phosphatase activity to recombinant human bone morphogenetic protein-2 (rhBMP2, ng/ml) (see Fig. 4B of Yoshida et al. [25]). The maximum rate of osteoid apposition, $V_{max,Ost}$, was reduced at each time step (equation 5 in Table 1) to represent the limitation imposed by the gradual differentiation of osteoblasts, which is accompanied by a reduction in nuclear height [3] and the amount of protein synthesising apparatus. This decline in activity is represented in the model by a daily reduction in the maximum velocity of osteoblast osteoid-forming activity of factor z, which has the same units as $V_{max,Ost}$. The value of z is 0.5 µm³/day during phase IV and 0.13 µm³/day during phase V. These values were found by comparing dynamic simulations to the matrix and mineral apposition rate data (see Fig. 7 of Eriksen et al. [3]) and relative changes in osteoid thickness, calcification rate, and matrix apposition rate (Fig. 8B,D,H of Eriksen et al. [3], respectively).

Phase IV is characterised by both osteoid formation and osteoid maturation, and there is an approximate 15-day "mineralisation lag time" before the new osteoid matrix is mature enough for mineralisation to start [3]. Mineralisation begins when the maximum depth of new osteoid in normal healthy bone reaches 16 µm (in agreement with Fig. 8B of Eriksen et al. [3]).

The rate of bone apposition can vary, depending on bone site, the proximity of blood vessels and red marrow cells, blood flow, and disease [2, 4, 26]. Also, the duration of bone apposition may vary with diseases such as hypoparathyroidism and hyperparathyroidism [20]. So it is unlikely that the demarcation of changing cellular events, such as the onset of mineralisation and osteocyte development, is defined by periods of time. It was therefore assumed for model purposes that the demarcation of cellular events was defined by matrix depth. The assumption that matrix depth rather than time interval triggers changes in cellular activity is supported by the possible role that osteocyte signalling may play in inhibiting bone apposition rates and thereby instigating osteocyte formation [27]. Marrotti (1996) suggested that when an osteocyte is sufficiently covered by new matrix, it signals the slowing down of bone formation. The osteoblast that receives the most signal therefore produces the least matrix, causing it to be buried by matrix produced by neighbouring osteoblasts, and so becomes an osteocyte [15, 27]. Therefore, rather than using a 15-day interval for the onset of mineralisation, it was assumed that mineralisation would begin once the newly formed osteoid had reached a maximum depth of 16 µm.

Phase V: Mineralisation and continued osteoid formation. During phase V, osteoblasts regulate the ordered deposition of mineral by producing cytokines such as osteocalcin and bone sialoprotein [28]. At the same time, osteoblasts continue to produce new osteoid, albeit at a reduced rate [3]. The amount of mineralised matrix at any one time during phase V (G_{Mz}) was calculated as the accumulated volume of mineralised matrix (A_{Mz}), which was computed on a daily time step (equation 6 in Table 1) from the rate of mineralisation (A_{Mz}), described by M-M kinetics (equation 7 in Table 1), where $V_{max,Mz}$ is the maximum velocity, s_{Mz} is the available substrate, $K_{m,Mz}$ is the M-M constant of mineralisation, and N is the number of cells. Values of the M-M parameters $V_{max,Mz}$, s_{Mz} and $K_{m,Mz}$ at the start of phase V were estimated from the initial rate of mineral apposition as illustrated in Figure 7 of Eriksen et al. [3].

In addition to mineralisation, osteoid formation continues during phase V. The rate of osteoid apposition was calculated by equation 3 (Table 1), the same relationship as that used for phase IV. The rate of osteoid apposition once mineralisation starts (at the start of phase V) is half of the original rate at the start of phase IV [3]. However, $V_{max,Ost}$ at the end of phase IV has been reduced by progressive reduction in cell volume during phase IV. We therefore propose that the estimated value of $V_{max,Ost}$ at the start of phase V cannot be equivalent to half of either its initial or its terminal values in phase IV, so we used two-thirds of its terminal value. Thus, $V_{max,Ost}$ at the start of phase V is not an input value. $V_{max,Minz}$, the maximum rate of mineralisation, however, is an input parameter. During phase V, osteoblasts continue to differentiate and flatten, reducing their cell volume, protein-synthesising apparatus, and matrix-forming efficiency [2, 4]. The assumed daily decrease in maximum capacity of osteoid formation during phase V was represented as a daily reduction in the value of $V_{max,Ost}$, by z_v (the cell size reduction factor, equation 5 in Table 1). The rate of reduction in $V_{max,Ost}$ was estimated by fitting simulation curves to matrix apposition growth curves together with relative changes in the osteoid apposition rate and the osteoid seam width, with time (as illustrated in Figs. 7 and 8B,H of Eriksen et al. [3]).

The process of simulation determined that the number of osteoblast cells at the microsite was reduced by 10 once the depth of mineralised matrix had reached 15, 30, and 45 µm, respectively. This reduction in cell number represents the number of osteocytes formed and incorporated within the matrix. The number of osteoblasts is not reduced gradually in the model, which is in keeping with the suggestion that it is the distance of osteoblasts from osteocytes within the matrix that may control which osteoblast is to become an osteocyte, by

Table 2. Model parameter symbols, values (unless calculated within model simulations), units in parentheses, description, and, where appropriate, source in square brackets

Term	Input parameter	Value (units)	Description and source
A_{Mz}		(μm^3/day)	Rate of mineralising osteoblast activity
A_{Ost}		(μm^3/day)	Rate of osteoid-forming cellular activity
G_{Ost}		(μm^3)	Volume of osteoid matrix formed
G_{Mz}		(μm^3)	Volume of mineralised matrix
$K_{m,Mz}$	I	135 (ng/ml)	M-M constant for mineralisation
$K_{m,Ost}$	I	90 (ng/ml)	M-M constant for osteoid formation
N			Number of cells
N_0	I	5	Number of committed osteoprogenitor cells at the start of the proliferative phase [18]
P_{Mz}		(days)	Duration of mineralising cellular activity
P_{Ost}		(days)	Duration of osteoid-forming activity
s_{Mz}		(μm^3)	Amount of osteoid substrate for mineralisation
$s_{Ost,0}$	I	200[a]	Amount of amino acid substrate for osteoid formation at start of phase IV
T	I	16 (hours)	Division time [18]
T		(days)	Time from start of phase IV
TGF-ß			Amount of TGF-ß released from matrix
$V_{max,Ost}$			Maximum velocity of osteoblast osteoid-forming activity
$V_{max,Ost,0}$	I	40 (μm^3/day)	Maximum velocity of osteoblast osteoid-forming activity at start of phase IV
$V_{max,Mz}$	I	22.33 (μm^3/day)	Maximum velocity of osteoblastic mineralisation activity at start of phase V (= two-thirds of $V_{max,Ost}$ at end of phase IV)
z_{IV}, z_V	I	0.5, 0.13 (μm^3/day)	Reduction in cell size factor for phases IV and V, respectively
α	I	0.75	Mitotic fraction [18]

I, model input parameters; [a,d] arbitrary and dimensionless units, respectively

becoming covered with matrix [15]. Therefore, as the matrix is laid down in lamellae, by a layer of osteoblasts at the surface, it was assumed that several osteoblasts of that layer might simultaneously reach the critical distance from embedded osteocytes. Furthermore, the number of active cells was also reduced by a further four cells per day, once the depth had reached 55 µm, to represent the increased rate of apoptosis of surplus osteoblasts towards the end of the formation period. The four cell/day reduction in cell number and the depth of 55 µm were incorporated into the model as they best simulated the reduction in the rate of apposition towards the end of the formation phase (Fig. 3). Although osteoblasts that are not surplus may undergo apoptosis, the data used for model construction did not include the timing and numbers of cells involved in such events. This simplification allowed investigation into the effects of a disruption in (1) the original number of cells which formed the team of osteoblasts at the end of proliferation and (2) the steady reduction in matrix apposition rate, by changing the value of the factor z that reduces the maximum capacity for osteoblast activity each day. At a later date, the model may be amended to enable the simulation of changing rates of apoptosis during any part of phases IV and V and not just the apoptosis of surplus cells towards the end of formation.

Model Testing and Sensitivity Analysis

In lieu of *in vivo* data for model testing, simulated matrix apposition rates were tested against data derived from histomorphometric techniques [29–31]. Although the model input factors, identified in Table 2, appeared to have fixed values in normal, healthy bone at one microsite, these values may change between bone sites or with disease [2, 26]. Therefore, it was appropriate to test how sensitive the depth and duration of bone apposition were to changes in the model input factors. These input variables were placed on the model input screen so that they could be readily changed by the operator, and the results were presented visually on the model output screen and

as data text files in the application's file directory. It is accepted that the validation of model input values will always be difficult, due to the inherent problem of studying bone, where any attempt to take measurements *in vivo* disrupts the process. Further, the numerical value of an input parameter is considered to be not so relevant as the change in its value on bone apposition, thus permitting a sensitivity analysis to be conducted by varying model input values. For the sensitivity analysis, control values of input parameters were increased and decreased by the following increments: 2%, 5%, and 10%. The results of changing the values of model input parameters of phase III, that is, the number of cells on day 1 of phase III (N_0), mitotic fraction (α), and division time (T), were expressed as a percent change in the number of cells 6 days later at the end of phase III (N). This affected bone apposition as well as the number of cells. The results of changing input parameters of phases IV and V affected bone apposition only.

Results

The "control" simulations of matrix apposition and mineralisation depth during phases IV and V of normal healthy bone remodelling at one microsite are illustrated by the dashed and solid lines of Figure 3, respectively. Phase IV began on day 50 and lasted for 15 days (Fig. 3). It consisted of osteoid formation and maturation but no mineralisation. The start of phase V was marked by the beginning of mineralisation of the mature osteoid, which occurred concurrently with continuing formation and maturation of new osteoid. Phase V lasted 135 days (Fig. 3).

Sensitivity analysis was conducted to determine how sensitive the model outputs were to changes in each model
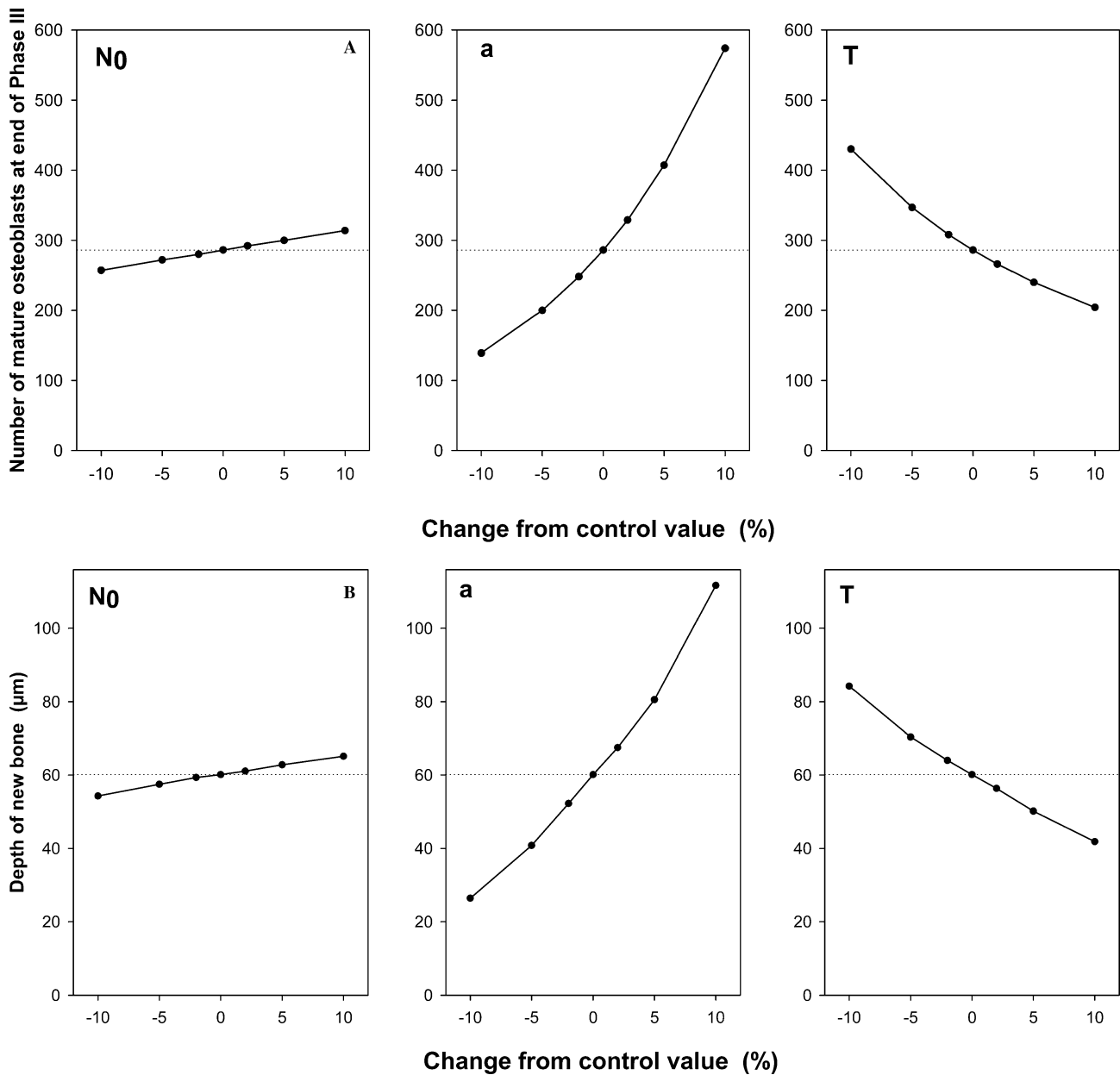
Fig. 4. Changes in the simulated number of mature osteoblasts formed at the end of phase III (**a**) and in the depth of new bone (**b**), when varying control values of the factors: number of osteoprogenitor cells (N_0), mitotic fraction (α), division time (T), by 2%, 5%, and 10%. Normal values are shown by *dotted line*.

input variable. The effects of changing input control values by ±10% are shown in Table 3 as percent changes in cell number, depth of new bone, depth of mineralisation, duration of formation, and percent mineralisation.

Phase III

The numbers of mature, osteoid-forming osteoblasts formed at the end of phase III were determined by equation 3 (Table 1). The three input parameters were the number of committed osteoprogenitor cells at the start of phase III (N_0), the mitotic fraction (α), and cell division time (T). The simulated depth of new bone was highly

sensitive to changes in the fraction of cells that were able to undergo mitosis during the reversal phase (α). A 10% increase caused a 100% increase in the number of mature osteoblasts formed and an 86% increase in bone depth (Table 3). Whereas a 10% decrease in mitotic fraction resulted in a decrease of about 50% in both number of cells and depth of bone formed, it also decreased duration of the formation phase by 15%. Bone apposition depth was also sensitive to cell division time, T. Increasing the division time T by 10% produced a 29% reduction in cell numbers and a 30% reduction in depth of bone formed (Table 3), whereas a 10% decrease in T led to a 50% increase in cell number at the end of phase III and a 40%

Table 3. Percentage change in simulated number of mature osteoblasts, depth of bone formed, duration of formation phase, and mineralisation, with a 10% change in control values of input variables

	Change in variable	Number of cells	Depth	Duration	Mineralisation
N_0	+10%	+9.8	+8.3	+1.5	+0.3
	−10%	−10.1	−9.7	−1.5	−0.3
α	+10%	+100.7	+85.8	+6.5	+0.6
	−10%	−51.4	−56.0	−15.5	−1.9
T	+10%	−28.7	−30.3	−5.5	−0.4
	−10%	+50.3	+40.2	+4.0	+0.6
$V_{max,Ost,0}$	+10%		+13.2	+12.0	+1.0
	−10%		−19.6	−12.0	−0.7
$K_{M,Ost}$	+10%		−2.8	0	−0.1
	−10%		+3.4	1.0	+0.2
$s_{Ost,0}$	+10%		+3.0	1.0	0.2
	−10%		−3.1	0	−0.1
z_{IV}	+10%		−2.5	−1.5	−0.1
	−10%		+2.5	+2.0	+0.2
z_V	+10%		−5.0	−6.0	−0.4
	−10%		+4.6	+7.5	+0.5
$V_{max,Mz}$	+10%		−0.3	0	+0.2
	−10%		+0.5	0	−0.4
$K_{m,Mz}$	+10%		0.1	0	−0.2
	−10%		−0.3	0	+0.2

increase in depth of new bone formed. However, the model was less sensitive to changes in the third parameter, which determines cell number: the number of committed osteoprogenitor cells at the start of the reversal phase (N_0). A 10% increase in N_0 led to an increase in cell number of 9.8% and an 8.3% increase in depth, whereas a 10% decrease produced a 10.1% decrease in cell numbers and a 9.7% decrease in depth of new bone (Table 3).

The effects of altering the normal, healthy (i.e., control) value of the three input parameters that affect rates of cell growth, α, T, and N_0, by 2%, 5%, and 10%, are illustrated in Figure 4a. The changes in mature osteoblast number led to changes in depth of bone formed (Fig. 4b). The dependence of depth on mature osteoblast numbers was nearly linear (Fig. 5).

Phases IV and V

Of the factors that affect focal bone formation during phases IV and V, bone apposition was most sensitive to changes in the input factor $V_{max,Ost,0}$ (the maximum rate of osteoblast activity at the start of phase IV). A 10% increase in $V_{max,Ost,0}$ caused a 13.2% increase in depth and an increase of 12% in duration time. A 10% decrease in $V_{max,Ost,0}$ produced a 19.6% reduction in depth of bone formed and a 12% decrease in duration time (Table 3). Percentage increases in the cell size factor of phase V (z_V), the M-M constant for osteoid formation ($K_{m,Ost}$), and cell size factor of phase IV (z_{IV}) caused only 5%, 3%, and 2.5% reductions in depth of bone formed, respectively (Fig. 6, Table 3). Changes in the maximum rate of mineralisation ($V_{max,Mz}$) and the M-M constant of mineralisation ($K_{m,Mz}$) of up to 10% had little effect on depth of new bone formed (Table 3).
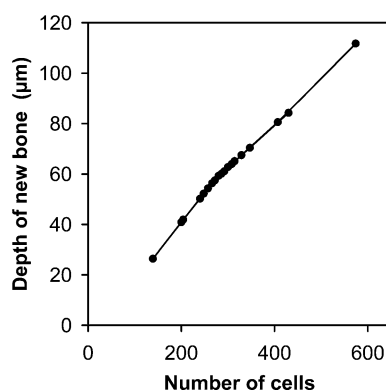

Fig. 5. Relationship between depth of bone formed and number of mature osteoblasts formed at the end of phase III, using data from Figure 4.

Although the duration of the formation phase was affected by changes in α, T, $V_{max,Ost,0}$, and z_V (Table 3), only a 10% increase in $V_{max,Ost,0}$, or a 10% reduction in division time caused a greater than 10% change in duration of formation phases (Table 3).

Sensitivity analysis showed the amount of matrix mineralised to be relatively well conserved, with 10% changes in model variables producing less than 2% changes in mineralisation (Table 3).

Discussion

Sensitivity analysis of the model showed the simulated depth of new bone formed to be highly dependent on cell number (Fig. 5) and not so dependent on the factors that determine cellular activity (Fig. 6). This is in agreement with the critical role that the regulation of
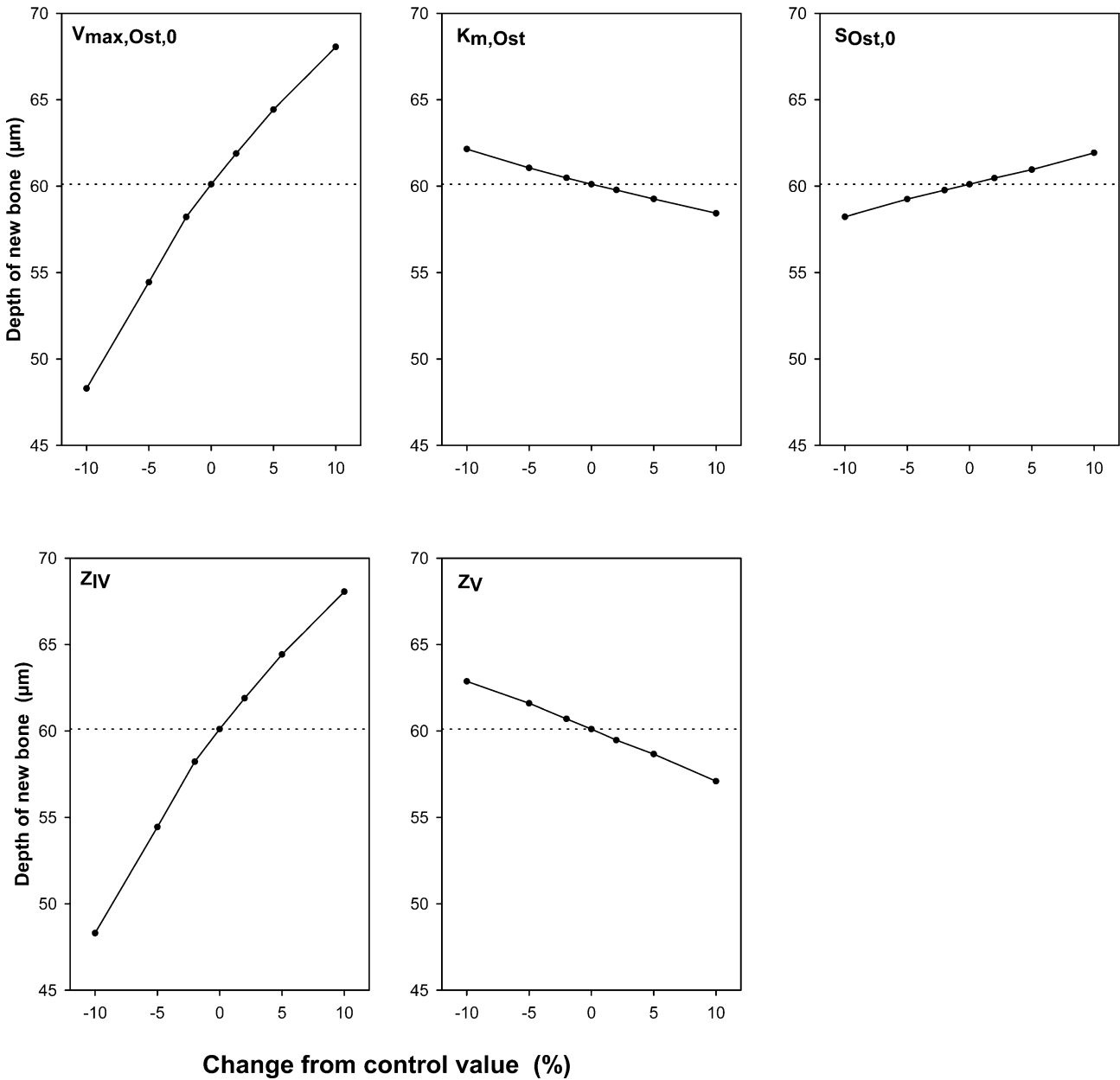
Fig. 6. Changes in depth of bone formed, simulated by varying input values by 2%, 5%, and 10% of the factors that affect phases IV and V: maximum rate of osteoid-forming activity at start of phase IV ($V_{max,Ost,0}$), M-M constant of osteoid-forming activity ($K_{m,Ost}$), substrate for osteoid formation ($s_{Ost,0}$), cell size reduction factor during phase IV (z_{IV}), and cell size reduction factor during phase V (z_V). (Changes in maximum rate of mineralisation, $V_{max,Mz}$, and M-M constant of mineralisation, $K_{m,Mz}$, not shown.) Depth of 60 μm is shown by *dotted line*.

preosteoblast proliferation is known to play in normal bone remodelling [1, 24]. The number of cells was particularly sensitive to changes in the fraction of the cell population able to undergo mitosis (α). Indeed, as little as a 2% increase in mitotic fraction gave a 15% increase in simulated cell number (Fig. 4a) and caused a 12.3% increase in depth of bone formed (Fig. 4b). The number of cells was also sensitive to cell division time, with a 2% decrease in T resulting in a 7.7% increase in cell number and a 6.4% increase in the amount of bone formed

(Fig. 4a,b). However, the depth of bone formed was relatively insensitive to changes in the number of committed osteoprogenitor cells at the start of phase III (N_0). A 2% change in N_0 caused a 2% change in cell numbers and a less than 2% change in bone depth (Fig. 4b).

Bone apposition was relatively insensitive to changes in the model factors that predicted the rate of cellular activity. Of these factors, bone depth was most sensitive to changes in the maximum capacity of osteoblast

activity at the start of phase IV ($V_{\mathrm{max,Ost,0}}$). Indeed, a 2% change in $V_{\mathrm{max,Ost,0}}$ only gave a 3% change in the amount of bone formed (Fig. 6). A 2% change in all other model factors that determined cellular activity produced a less than 2% change in bone depth.

The model provides flexibility in understanding because it can incorporate factors that alter the apposition process. This is shown by the results of the sensitivity analysis that reflect the dependence of bone formation depth on osteoblast number and, thus, indicate the requirement for stringent regulation of proliferation during the "coupled" remodelling of healthy young adult cancellous bone, where the amount of new bone formed exactly replaces the amount of bone removed by prior resorption. Although the mechanisms that control cell number during coupled remodelling are highly complex and not fully understood, growth factors that are released from the bone matrix during resorption, such as TGF-β and BMPs, are thought to play a major signalling role [24]. Different local factors might be expected to play distinct roles in cell growth, which may be simulated in the model by their effects on two processes: firstly, on the number of osteoprogenitor cells and, secondly, on the rate of proliferation of preosteoblasts. Factors released during resorption might be expected to recruit osteoprogenitor cells from mesenchymal stem cells in the local bone marrow microenvironment. Committed osteoprogenitor cells are attracted to the bone surface by a combination of chemotactic factors within the matrix, including type-1 collagen, osteocalcin, TGF-β, and PDGF [24]. As the proliferation of committed osteoprogenitor cells during coupled remodelling is delayed until the cells have migrated to the matrix surface, the onset and rate of proliferation might be expected to be regulated by matrix signalling, including signals from the network of osteocytes. Therefore, it is assumed that the control of cell number by released growth factors and chemotactic factors within the matrix can be simulated in the model via their effects on the number of committed osteoprogenitor cells at the surface of the bone matrix at the start of proliferation (N_0). As the osteoprogenitor cells arrive at the bone surface, they start to differentiate into preosteoblasts. Therefore, the regulation of proliferation of preosteoblasts by local matrix signalling during coupled remodelling can presumably be simulated by their effects on two model factors: (1) the fraction of cells that are mitotic (α) and (2) division time (T). To summarise, the model simulates the maximum number of active cells that form bone during normal "coupled" remodelling from (1) the number of committed osteoprogenitor cells (N_0), which is assumed to be controlled by the growth factors released from the matrix and chemotactic factors, and (2) the fraction of cells that can undergo mitosis (α) together with their division time (T), which are assumed to be controlled by matrix signals, including those from the osteocyte network. Systemic and extraneous signalling, such as that which occurs with changes in hormone levels or with disease, may disrupt the tight regulation of cell numbers and cellular activity of the normal remodelling cycle. Disruption may also affect the activation frequency of remodelling events.

Future work is planned to improve model capability. This includes an increased biological basis for simulating the matrix maturation and mineralisation processes, to allow the simulation of significant changes in rates of mineralisation together with a more complex representation of apoptotic cell death during formation, to enable the simulation of growth factor-inhibited apoptosis. Further work will use the model to compare predicted outcomes with actual data, for example, to simulate the effects of age on bone formation via age-related decreases in the number of osteoprogenitor cells.

The model predicts rates of bone apposition and mineralisation that are in agreement with independent data presented elsewhere in the literature. For example, mean apposition and mineralisation rates are 0.41 and 0.45 μm/day, respectively, which correspond to the mineral apposition rates that have been measured by tetracycline labelling of 0.50 ± 0.10 μm/day in younger women [29] and 0.52 ± 0.9 μm/day in normal adult iliac trabecular bone [30]. However, the simulated mineralisation rate of 0.45 μm/day was lower than the 0.66 μm/day measured by Charles et al. [31]. In addition, the bone formation period was simulated to last 150 days, which was the same as the data obtained by Charles et al. [31].

This model was constructed based on the data of Eriksen et al. [3], and because of the use of dynamic equations to simulate cell proliferation and cellular activity, the model can be adapted to simulate different rates of apposition. This model is a simplified and adaptable representation of the apposition of bone during coupled remodelling. It can also be used to aid greater understanding of the mechanisms that underlie focal bone formation and to predict the effects of disruption on the system. The model may be used to simulate how different concentrations and combinations of growth factors and cytokines might affect bone apposition at different bone sites in normal bone through effects on cell number, for example, with proximity to red bone marrow [2]. In addition, the model may be used to simulate bone apposition in the absence of bone matrix and osteocyte signalling, for example, when osteoblasts are transferred to sites of the body where other stem cells occur (ectopic calcification) or *in vitro* in the presence of TGF-β and BMPs via the effects of growth factor and cytokine signalling on the three model factors that determine proliferation rate (mitotic fraction, α division time, T; and number of committed osteoprogenitor cells, N_0).

Indeed, the high sensitivity of bone apposition to number of cells helps to explain how a change in signalling within the bone microenvironment, whether from bone cells or other cells, which cause a change in concentrations of mitogenic growth factors or cytokines, could overcome the limiting factors that regulate bone formation during normal coupled remodelling. A gross change in mechanical forces acting on bone may lead to uncoupling and an imbalance in the remodelling process. For example, a sustained increase in loading at a skeletal site, as might occur with an increase in physical exercise, could cause increased bone formation *in vivo*. During remodelling of trabeculae at such sites, the amount of bone formed would exceed the amount of bone resorbed. Even relatively small increases in osteogenic mitogens could lead to substantial increases in the number of osteogenic cells and, hence, bone formation under appropriate conditions. Abnormal rates of bone formation can occur in bone disease where signalling is altered by cells within the marrow cavity, such as marrow macrophages and T cells [24]. Also, even more dramatic increases in bone formation rates can be caused by the signalling of osteogenic tumour cells within bone metastases [32].

In summary, this simple model of bone apposition, although limited by the paucity of *in vivo* data, can simulate changes in bone apposition rates via alterations in cell number and activity. It can also help to explain how the homeostatic processes of bone resorption and formation seen during coupled remodelling can be disrupted, particularly by factors that affect the mitotic fraction and division time of proliferative preosteoblast cells.

References

1. Parfitt AM (1994) Osteonal and hemi-osteonal remodeling: the spatial and temporal framework for signal traffic in adult human bone. J Cell Biochem 55:273–286
2. Ott SM (2002) Histomorphometric analysis of bone remodeling. In: Bilezikian JP, Raisz LG, Rodan GA (eds) Principles of bone biology, 2nd ed vol 1. Academic Press, San Diego, pp 303–319
3. Eriksen EF, Gundersen HJG, Melsen F, Mosekilde L (1984) Reconstruction of the formative site in iliac trabecular bone in 20 normal individuals employing a kinetic model for matrix and mineral apposition. Metab Bone Dis Relat Res 5:243–252
4. Parfitt AM (1984) The cellular basis of bone remodelling: the quantum concept reexamined in light of recent advances in the cell biology of bone. Calcif Tissue Int 36:S37–S45
5. Sunray M, Zurgil N, Shafran Y, Deutsch M (2002) Determination of individual cell Michaelis-Menten constants. Cytometry 47:8–16
6. Boonacker EP, Wierenga EA, Smits HH, Van Noorden CJF (2002) CD26/DPPIV signal transduction function, but not proteolytic activity, is directly related to its expression level on human Th1 and Th2 cell lines as detected with living cell cytochemistry. J Histochem Cytochem 50:1169–1177
7. Farquahar GD, von Caemmerer S, Berry JA (1980) A biochemical model of photosynthetic CO_2 assimilation in leaves of C_3 species. Planta 149:78–90
8. von Caemmerer S, Farquhar GD (1981) Some relationships between the biochemistry of photosynthesis and the gas exchange of leaves. Planta 153:376–387
9. Long SP (1991) Modification of the response of photosynthetic productivity to rising temperature by atmospheric CO_2 concentrations: has its importance been underestimated?. Plant Cell Environ 14:729–739
10. Martin MJ, Farage PK, Humphries SW, Long SP (2000) Can the stomatal changes caused by acute ozone exposure be predicted by changes occurring in the mesophyll? A simplification for models of vegetation response to the global increase in tropospheric elevated ozone episodes. Aust J Plant Physiol 27:211–219
11. Martin MJ, Stirling CM, Humphries SW, Long SP (2000) A process-based model to predict the effects of climatic change on leaf isoprene emission rates. Ecol Mod 131:161–174
12. Martin MJ, Host GE, Lenz KE, Isebrands JG (2001) Simulating the growth response of aspen to elevated ozone: a mechanistic approach to scaling a leaf-level model of ozone effects on photosynthesis to a complex canopy architecture. Environ Pollut 115:425–436
13. Hernandez CJ, Beaupré GS, Carter DR (2003) A theoretical analysis of the changes in basic multicellular unit activity at menopause. Bone 32:357–363
14. Huiskes R, Ruimerman R, van Lenthe GH, Janssen JD (2000) Effects of mechanical forces on maintenance and adaptation of form in trabecular bone. Nature 405:704–706
15. Martin RB (2000) Does osteocyte formation cause the nonlinear refilling of osteons? Bone 26:71–78
16. van der Linden JC, Verhaar AN, Weinans H (2001) A three-dimensional simulation of age-related remodeling in trabecular bone. J Bone Miner Res 16:688–696
17. Martin MJ, Buckland-Wright JC (2004) Sensitivity analysis of a novel mathematical model identifies factors determining bone resorption rates. Bone 35:918–928
18. Deasy BM, Qu-Peterson Z, Greenberger JS, Huard J (2002) Mechanisms of muscle stem cell expansion with cytokines. Stem Cells 20:50–60
19. Parfitt AM (2002) The bone remodeling compartment: a circulatory function for bone lining cells. J Bone Miner Res 16:1583–1585
20. Eriksen EF, Axelrod DW, Melsen F (1994) Bone histomorphometry. Raven Press, New York, pp 13–20
21. Parfitt AM (2002) Targeted and nontargeted bone remodeling: relationship to basic multicellular unit origination and progression. Bone 30:5–7
22. Hernandez CJ, Beaupré GS, Carter DR (2000) A model of mechanobiologic and metabolic influences on bone adaptation. J Rehab Res Dev 37:235–244
23. Baron R (1999) Anatomy and ultrastructure of bone. In: Favus MJ (ed) Primer on the metabolic bone diseases and disorders of mineral metabolism. Lippincott Williams and Wilkins, London, pp 3–10
24. Mundy GR, Chen D, Oyajobi BO (2003) Bone remodeling. In: Favus MJ (ed) Primer on the metabolic bone diseases and disorders of mineral metabolism. American Society for Bone and Mineral Research, Washington DC, pp 46–58
25. Yoshida Y, Tanaka S, Umemori H, Minowa O, Usui M, Ikematsu N, Hosoda E, Imamura T, Kuno J, Yamashita T, Miyazono K, Noda M, Noda T, Yamamoto T (2000) Negative regulation of BMP/Smad signaling by Tob in osteoblasts. Cell 103:1085–1097
26. Reeve J, Arlot ME, Chavassieux PM, Edouard C, Green JR, Hesp R, Tellez M, Meunier PJ (1987) The assessment of bone formation and bone resorption in osteoporosis: a comparison between tetracycline-based iliac histomorph-

ometry and whole body 85Sr kinetics. J Bone Miner Res 2:479–489
27. Marrotti G (1996) The structure of bone tissues and the cellular control of their deposition. Ital J Anat Embryol 101:25–79
28. Lian JB, Stein GS, Canalis E, Robey PG, Boskey AL (1999) Bone formation: osteoblast lineage cells, growth factors, matrix proteins, and the mineralization process. In: Favus MJ (ed) Primer on the metabolic bone diseases and disorders of mineral metabolism. Lippincott Williams and Wilkins, London, pp 14–29
29. Eastell R, Delmas PD, Hodgson SF, Eriksen EF, Mann KG, Riggs BL (1988) Bone formation rate in older normal women: concurrent assessment with bone histomorphometry, calcium kinetics and biochemical markers. J Clin Endocrinol Metab 67:741–748
30. Melsen F, Mosekilde L (1978) Tetracycline double-labeling of iliac trabecular bone in 41 normal adults. Calcif Tissue Res 26:99–102
31. Charles P, Eriksen EF, Moskilde L, Melsen F, Jensen FT (1987) Bone turnover and balance evaluated by a combined calcium kinetic study and dynamic histomorphometry. Metabolism 36:1118–1124
32. Chirgwin JM, Guise TA (2003) Cancer metastasis to bone. Sci Med 9:140–151